REGIMES OF INTERACTIONS BETWEEN EXPANDING PREMIXED FLAMES AND TOROIDAL VORTICES

V. Di Sarli and A. Di Benedetto
valeria.disarli@irc.cnr.it
Istituto di Ricerche sulla Combustione - Consiglio Nazionale delle Ricerche (IRC-CNR), Via Diocleziano 328, 80124, Napoli, Italy

Abstract
In this paper, the regimes of interactions between premixed flame fronts and toroidal vortex structures generated at the wake of a circular orifice have been quantified on the spectral diagram by Vasudeo et al. (Phys. Fluids 22, 043602, 2010), using the experimental data acquired by Long et al. (J. Phys. Conf. Ser. 45, 104-111, 2006) for different orifice diameters (20 mm, 30 mm and 40 mm). As the orifice diameter decreases, both size and velocity of the vortex increase. This, in turn, increases the intensity of the flame-vortex interaction, leading to a transition through different regimes. It has been found that the flame-vortex interaction occurs inside the wrinkled regime at the wake of the 40 mm orifice, inside the breakthrough regime at the wake of the 20 mm orifice and at the boundary between wrinkled and breakthrough regimes at the wake of the 30 mm orifice. The identification of such regimes is consistent with the observation of the flame behavior. This provides a first assessment of the reliability of the spectral diagram.

Introduction
The dynamic interaction that occurs between a propagating premixed flame front and a rotating vortex structure is one of the key mechanisms within turbulent combustion. As such, it is found within many applications (e.g., industrial combustors and burners, internal combustion engines, obstacle-induced explosions, etc.). The manner in which the flame propagates through a turbulent flow field and, thus, the combustion regime experienced by the flame are strictly dependent on both size and velocity (i.e., strength) of the vortical structures encountered.

Early diagrams defining combustion regimes for turbulent premixed flames in terms of length and velocity scales have been proposed by Barrère [1], Bray [2], Borghi [3], Williams [4] and Peters [5]. These diagrams, which are essentially phenomenological, have evolved into spectral diagrams obtained from analyses of the effects of individual turbulence scales on the flame response [6-10]. Flame-vortex interactions are common configurations for these studies. In particular, planar flame-vortex configurations have widely been employed.

An extension of the planar configuration is the flame kernel-vortex (KV) configuration, first presented by Eichenberger and Roberts [11], in which vortices more realistically interact with an expanding flame kernel. Regimes of KV interactions have been studied in both experimental [11-13] and computational [14-17] works. Five distinct regimes have been identified: (1) the laminar kernel regime, (2) the wrinkled kernel regime, (3) the breakthrough regime, (4) the global extinction regime and (5) the regeneration after global extinction (RGE) regime. Increasing the vortex size and velocity leads to a gradual transition through regimes (1-4).

In the laminar kernel regime, vortices are too small and/or weak to alter the structure and dynamics of the flame kernel. The wrinkled kernel regime is characterized by significant distortion (wrinkling) of the flame kernel. In the breakthrough regime, vortices are strong enough to produce the splitting of the flame kernel into two kernels, which may eventually

connect with each other, giving rise to a single deformed kernel. In the global extinction regime, the global straining of the flame kernel causes its extinction. Finally, in the RGE regime, reignition takes place after most of the initial kernel has extinguished due to intense straining.

A regime diagram for KV interactions has been built by Echekki and Kolera-Gokula [15] and recently revisited by Vasudeo et al. [16]. The revisited diagram is shown in Figure 1. It allows quantifying regimes (1-5) in terms of two key parameters evaluated at the beginning of the interactions. These parameters correspond to the ratio of the vortex radius to the flame kernel radius (x-axis), R_v/R_f, and the ratio of the maximum vortex rotational velocity to the laminar burning velocity (y-axis), $u_{\theta,max}/S_L$.

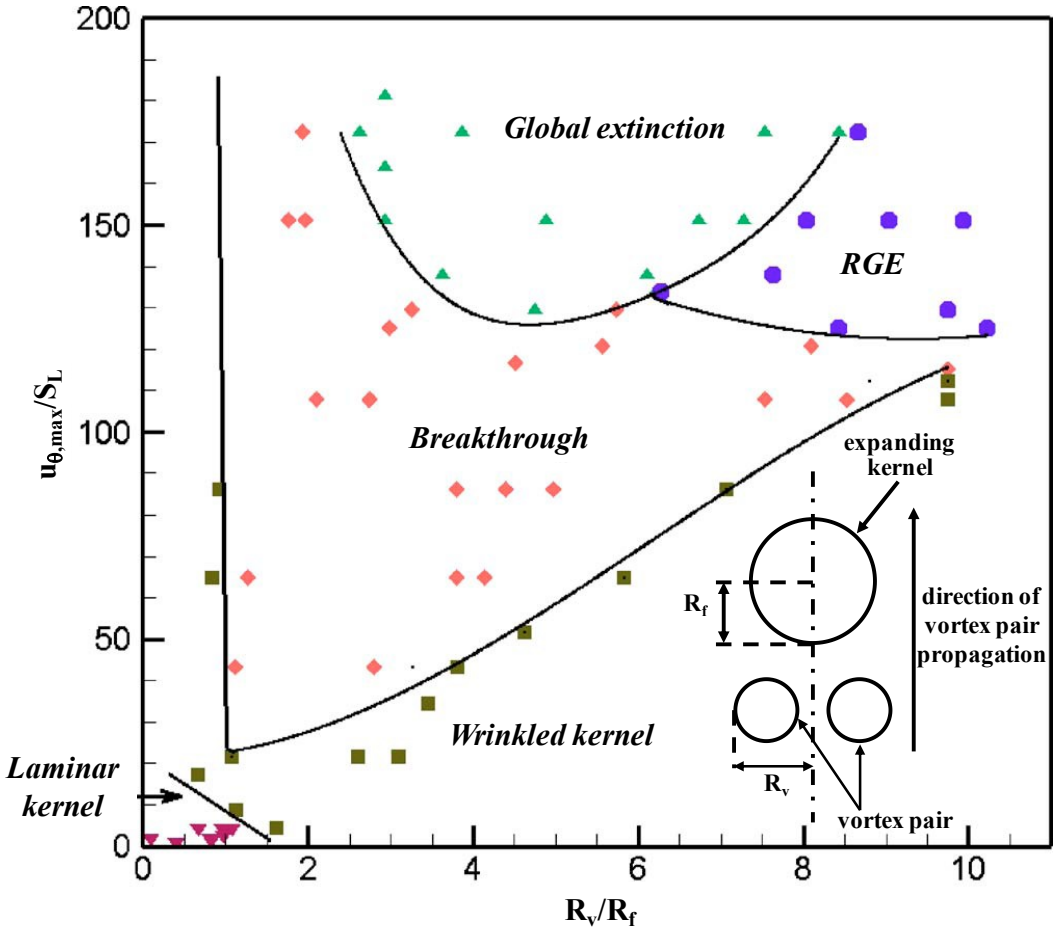

Figure 1. Spectral diagram for flame kernel-vortex interactions by Vasudeo et al. [16] (the schematic of the computational configuration used is also shown).

The diagram of Figure 1 (as well as the diagram originally presented by Echekki and Kolera-Gokula [15]) has been constructed from direct numerical simulations of interactions between a post-ignition flame kernel and a counter-rotating vortex pair. Computations were implemented in a simplified axisymmetric configuration (Figure 1). The diagram contains a great number of numerical results (represented by symbols) that provide the boundaries between the five regimes (reverse triangles: laminar kernel regime; squares: wrinkled kernel regime; diamonds: breakthrough regime; triangles: global extinction regime; circles: RGE regime). However, it has not yet been "validated" against experimental data.

In this paper, we make a first attempt to assess the reliability of the spectral diagram by Vasudeo et al. [16]. To this end, we selected the laser diagnostic data acquired by Long et al. [18] during transient interactions between expanding premixed flame fronts and simple

toroidal vortex structures generated at the wake of a circular orifice in a controlled manner. Such data cover a range of vortex scales and strengths. They consist of high-speed video recordings of the flame front temporal development (which allow the visualization of the flame response) and measurements of the velocity field of the unburned mixture ahead of the propagating front (which allow the quantification of the vortex size and velocity).

Experiments by Long et al. [18]

Long et al. [18] carried out experiments using the test rig schematized in Figure 2a. Within this rig, a quiescent premixed charge of stoichiometric methane and air was ignited inside a small cylindrical pre-chamber (35 mm in height and 70 mm in diameter) linked to the main chamber (150 mm x 150 mm x 150 mm) via a small orifice. The bottom end of the pre-chamber was fully closed. The upper end of the main chamber was sealed by a thin PVC membrane that ruptured soon after ignition, allowing the exhaust gases to escape. The main chamber was constructed from polycarbonate to provide optical access.

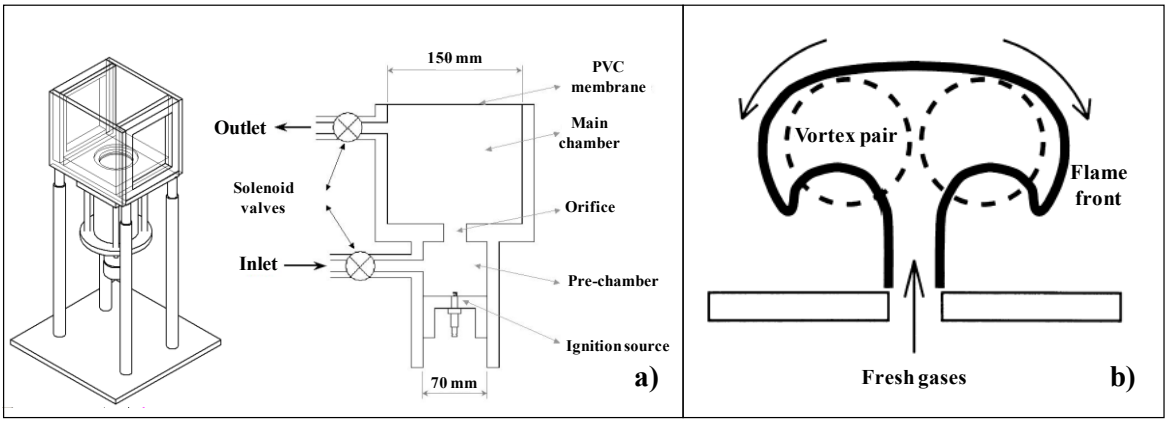

Figure 2. Schematics of the test rig by Long et al. [18] (not to scale) (a) and of the flame-vortex interaction (b).

Ignition was provided at the center of the bottom end of the pre-chamber. After ignition, the flame propagated through the pre-chamber, pushing unburned charge ahead of the flame front through the orifice. This motion of the reactants through the constriction resulted in a toroidal vortex being shed into the main chamber. As the flame continued to propagate through the charge, it interacted with the vortex structure, distorting the flame and altering its burning velocity. Figure 2b shows a two-dimensional sketch of the flame-vortex interaction (the toroidal vortex is schematized as a vortex pair).

The nature (size and velocity) of the vortices produced in the main chamber is strongly dependent on the orifice diameter. Three different orifice diameters were tested: 20 mm, 30 mm and 40 mm. All three orifices had a constriction length of 30 mm, with sharp edges at both the pre-chamber and main chamber sides.

In order to characterize the interaction between the flow field and the flame front, two high-speed laser diagnostic techniques were employed: High Speed Laser Sheet Flow Visualization (HSLSFV) and High Speed Digital Particle Image Velocimetry (HSDPIV). The HSLSFV technique provided a global visualization of the flame front development throughout the combustion event. The HSDPIV technique provided detailed velocity data (two-dimensional vector velocity maps) for the flow field into which the flame front burned.

Regimes of flame-vortex interactions for different orifice diameters

To quantify the regimes of flame-vortex interactions for different orifice diameters, we entered the diagram by Vasudeo et al. [16] with the values of R_v and $u_{\theta,max}$ extracted from the

HSDPIV data acquired by Long et al. [18] at the onset of the interaction. These values are given in Table 1 for all orifice diameters. The R_v/R_f and u_θ^{max}/S_L ratios are also reported in the table as computed setting the flame radius, R_f, equal to the orifice radius and the laminar burning velocity, S_L, equal to 0.41 m/s [19]. Both ratios increase with decreasing orifice diameter.

Table 1. Vortex radius, R_v, maximum vortex rotational velocity, $u_{\theta,max}$, vortex radius-to-flame radius, R_v/R_f, and maximum vortex rotational velocity-to-laminar burning velocity ratio, u_θ^{max}/S_L, as obtained for different orifice diameters

	R_v [mm]	$u_{\theta,max}$ [m/s]	R_v/R_f	$u_{\theta,max}/S_L$
20 mm	22.8	18	2.28	43.9
30 mm	25.6	11	1.71	26.8
40 mm	33	6	1.65	14.6

The points corresponding to the dimensionless ratios of Table 1 are included in the spectral diagram (rectangles, Figure 3).

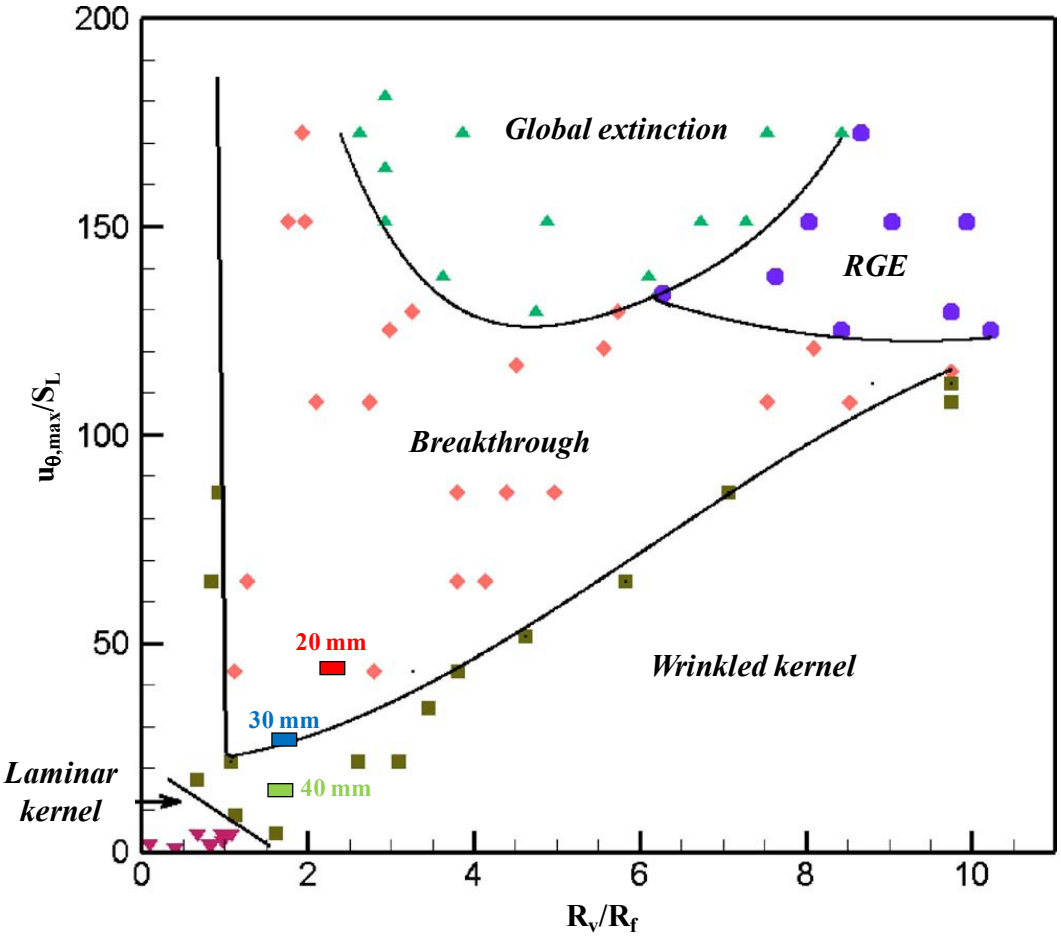

Figure 3. Spectral diagram for flame kernel-vortex interactions by Vasudeo et al. [16] including the current results for different orifice diameters (rectangles).

The flame-vortex interaction occurs inside the wrinkled regime at the wake of the 40 mm orifice, inside the breakthrough regime at the wake of the 20 mm orifice and at the boundary

between wrinkled and breakthrough regimes at the wake of the 30 mm orifice. This is consistent with the evolution of the flame behaviour shown by the images from the HSLSFV recordings. As the orifice size decreases, the intensity of the flame-vortex interaction increases: in the 40 mm case, the vortex only wrinkles the flame front; in the 20 mm case, the vortex disrupts the continuity of the front, giving rise to the formation of a separate reaction zone, which eventually merges with the main front; in the 30 mm case, the vortex essentially wrinkles the flame, however, it also produces a slight perturbation of the front structure.

Conclusions

The regimes of interactions between premixed flame fronts and toroidal vortex structures generated at the wake of a circular orifice have been quantified on the spectral diagram by Vasudeo et al. [16], using the experimental data acquired by Long et al. [18] for different orifice diameters (20 mm, 30 mm and 40 mm).

As the orifice diameter decreases, both size and velocity of the vortex increase. This, in turn, increases the intensity of the flame-vortex interaction, leading to a transition through different regimes. It has been found that the flame-vortex interaction occurs inside the wrinkled regime at the wake of the 40 mm orifice, inside the breakthrough regime at the wake of the 20 mm orifice and at the boundary between wrinkled and breakthrough regimes at the wake of the 30 mm orifice. The identification of such regimes is consistent with the observation of the flame behavior. This provides a first assessment of the reliability of the spectral diagram.

Our ongoing efforts are focused on the development of a Large Eddy Simulation (LES) model of transient flame-vortex interactions. We will validate the LES model against the experimental data by Long et al., verifying whether it grasps the transition between wrinkled and breakthrough regimes on the spectral diagram. Once validated, the LES model will provide results from which we will quantify three-dimensional features associated to the regime transition.

Acknowledgments

The authors gratefully acknowledge Professor Gennaro Russo for stimulating and fruitful discussions.

References

[1] Barrère, M., “Modèles de combustion turbulente”, *Rev. Générale de Thermique* 148:295-308 (1974).

[2] Bray, K.N.C., “Turbulent flows with premixed reactants”, In: Libby, P.A., Williams, F.A., editors, *Turbulent Reacting Flows*, volume 44 of *Topics in Applied Physics*, pp. 115-183, Springer-Verlag, 1980.

[3] Borghi, R., “On the structure and morphology of turbulent premixed flames”, In: Casci, C., Bruno, C., editors, *Recent Advances in the Aerospace Sciences*, pp. 117-138, Plenum Publishing Corporation, 1985.

[4] Williams, F.A., *Combustion Theory*, 2nd edition, Addison-Wesley, 1985.

[5] Peters, N., “Laminar flamelet concepts in turbulent combustion”, *Proc. Comb. Inst.* 21: 1231-1250 (1986).

[6] Meneveau, C., Poinsot, T., “Stretching and quenching of flamelets in premixed turbulent combustion,” *Comb. Flame* 86:311-332 (1991).

[7] Poinsot, T., Veynante, D., Candel, S., “Quenching processes and premixed turbulent combustion diagrams”, *J. Fluid Mech.* 228:561-606 (1991).

[8] Roberts, W.L., Driscoll, J.F., “A laminar vortex interacting with a premixed flame: Measured formation of pockets of reactants,” *Comb. Flame* 87:245-256 (1991).

[9] Roberts, W.L., Driscoll, J.F., Drake, M.C., Goss, L.P., "Images of the quenching of a flame by a vortex - To quantify regimes of turbulent combustion," *Comb. Flame* 94:58-69 (1993).
[10] Renard, P.-H., Rolon, J.C., Thévenin, D., Candel, S., "Wrinkling, pocket formation, and double premixed flame interaction processes," *Proc. Comb. Inst.* 27:659-666 (1998).
[11] Eichenberger, D.A., Roberts, W.L., "Effect of unsteady stretch on spark-ignited flame kernel survival", *Comb. Flame* 118:469-478 (1999).
[12] Xiong, Y., Roberts, W.L., Drake, M.C., Fansler, T.D., "Investigation of pre-mixed flame-kernel/vortex interactions via high-speed imaging", *Comb. Flame* 126:1827-1844 (2001).
[13] Xiong, Y., Roberts, W.L., "Observations on the interaction between a premixed flame kernel and a vortex of different equivalence ratio", *Proc. Comb. Inst.* 29:1687-1693 (2002).
[14] Kolera-Gokula, H., Echekki, T., "Direct numerical simulation of premixed flame kernel-vortex interactions in hydrogen-air mixtures", *Comb. Flame* 146:155-167 (2006).
[15] Echekki, T., Kolera-Gokula, H., "A regime diagram for premixed flame kernel-vortex interactions", *Phys. Fluids* 19:043604 (2007).
[16] Vasudeo, N., Echekki, T., Day, M.S., Bell, J.B., "The regime diagram for premixed flame kernel-vortex interactions - Revisited", *Phys. Fluids* 22:043602 (2010).
[17] Reddy, H., Abraham, J., "A numerical study of vortex interactions with flames developing from ignition kernels in lean methane/air mixtures", *Comb. Flame* 158:401-415 (2011).
[18] Long, E.J., Hargrave, G.K., Jarvis, S., Justham, T., Halliwell, N., "Characterisation of the interaction between toroidal vortex structures and flame front propagation", *J. Phys. Conf. Ser.* 45:104-111 (2006).
[19] Yu, G., Law, C.K., Wu, C.K., "Laminar flame speeds of hydrocarbon + air mixtures with hydrogen addition", *Comb. Flame* 63:339-347 (1986).